

# Pointwise vanishing velocity helicity of a flow does not preclude magnetic field generation

Alexander Andrievsky,<sup>1</sup> Roman Chertovskih,<sup>2</sup> and Vladislav Zheligovsky<sup>1</sup>

<sup>1</sup>*Institute of Earthquake Prediction Theory and Mathematical Geophysics,  
Russian Ac. Sci., 84/32 Profsoyuznaya St, 117997 Moscow, Russian Federation*  
<sup>2</sup>*Research Center for Systems and Technologies (SYSTEC), Faculty of Engineering,  
University of Porto, Rua Dr. Roberto Frias, s/n, 4200-465, Porto, Portugal*

Pointwise zero velocity helicity density is shown not to prevent steady flows from acting as kinematic dynamos. We present numerical evidences that such flows can generate both small-scale magnetic fields as well as, by the magnetic  $\alpha$ -effect or negative eddy diffusivity mechanisms, large-scale ones. The flows are constructed as curls of analytically defined space-periodic steady solenoidal flows, whose vorticity helicity (i.e., kinetic helicity) density is everywhere zero.

## I. INTRODUCTION

By a general mathematical definition, the helicity  $\mathcal{H}_f$  of a solenoidal zero-mean field  $\mathbf{f}(\mathbf{x}) = \nabla \times \Phi(\mathbf{x})$  is the spatial integral of the scalar product of the field and its vector potential  $\Phi$ . When both fields are space-periodic, the cell periodicity being the cube  $\mathbb{T} = [0, 2\pi]^3$ ,

$$\mathcal{H}_f = \int_{\mathbb{T}} \mathbf{f}(\mathbf{x}) \cdot \Phi(\mathbf{x}) \, d\mathbf{x}. \quad (1)$$

This quantity characterizes the knottedness of the field lines of the field  $\mathbf{f}$  [1]. Thus, helicities of different solenoidal flow-related fields (for instance, the flow  $\mathbf{v}$  itself and the vorticity  $\boldsymbol{\omega} = \nabla \times \mathbf{v}$ ) constitute a set of parameters measuring the flow complexity.

The magnetic  $\alpha$ -effect is supposed to play an important role in generation of cosmic and planetary magnetic fields. It is a manifestation of the interaction of fluctuating small-scale components of the field and velocity of the generating flow [2]. Heuristically, a generating flow  $\mathbf{v}$  is likely to have an intricate spatial structure featuring considerable knottedness of lines of the flow-related fields (implying, by virtue of the magnetic induction equation, that the magnetic field also has a nontrivial small-scale structure), the respective helicities not vanishing.

In the dynamo studies, a prominent quantity is the *vorticity helicity*  $\mathcal{H}_\omega$  (often referred to as *kinetic helicity*). It is a hydrodynamic invariant [3, 4] of ideal fluid flow, constraining the topology of vorticity lines [1]. The latter are a classical object described by the Helmholtz theorems. The discovery [5], that the helicity spectrum

$$H_{\mathbf{m}}(\mathbf{v}) = \widehat{\mathbf{v}}_{\mathbf{m}} \cdot (i\mathbf{m} \times \widehat{\mathbf{v}}_{\mathbf{m}}) \quad (2)$$

(a pedantic note: in line with the general definition of helicity of vector fields, it is logical to call it *the vorticity helicity spectrum*), where  $\widehat{\mathbf{v}}_{\mathbf{m}}$  are the Fourier coefficients of the flow,

$$\mathbf{v}(\mathbf{x}) = \sum_{\mathbf{m}} \widehat{\mathbf{v}}_{\mathbf{m}} e^{i\mathbf{m} \cdot \mathbf{x}},$$

is crucial for the presence of the  $\alpha$ -effect in the limit of small magnetic Reynolds numbers, has triggered many studies trying to establish links between  $\mathcal{H}_\omega$  and the flow dynamo properties (see also [6]). However, the ability of

a flow to generate magnetic field does not require its vorticity helicity density to be non-zero in the physical (the Christopherson flow is a counterexample [7]) or Fourier spaces (see [8] for an example of a generating flow with a zero helicity spectrum). Recently, a large variety of steady solenoidal flows with a pointwise zero vorticity helicity and zero helicity spectrum were shown [9] to act as kinematic magnetic dynamos generating small-scale magnetic fields and, by the mechanisms of the magnetic  $\alpha$ -effect and eddy (“turbulent”) diffusivity, large-scale ones.

However, the knottedness of fluid particle trajectories is directly characterized by the *velocity helicity*  $\mathcal{H}_v$  of the flow, rather than by the vorticity helicity  $\mathcal{H}_\omega$ , and thus the quantity  $\mathcal{H}_v$  may be closer related to the dynamo properties of flows (for instance, due to the frozenness of magnetic field in the ideal magnetohydrodynamics, see [10]).

For turbulent flows, in the low conductivity limit the  $\alpha$ -effect is proportional to the velocity helicity  $\mathcal{H}_v$  [11] (see also [12]). Generation of large-scale fields by the  $\alpha$ -effect was considered in [13] under assumptions in the spirit of the second-order correlation approximation, and the results were supposed to be reliable for small magnetic Reynolds numbers. The authors concluded that while for flows varying rapidly in time the vorticity helicity  $\mathcal{H}_\omega$  is the quantity crucial for the presence of the  $\alpha$ -effect, for steady ones the velocity helicity  $\mathcal{H}_v$  is crucial. Motivated by this statement, the present paper is devoted to a study of this conjecture by considering small- and large-scale dynamos for steady flows, whose velocity helicity density vanishes everywhere in space.

A comment is in order: The potential  $\Phi(\mathbf{x})$  of a field  $\mathbf{f}(\mathbf{x}) = \nabla \times \Phi(\mathbf{x})$  is defined up to an arbitrary gradient. While the helicity (1) is gauge-independent [1], the helicity density  $\mathbf{f}(\mathbf{x}) \cdot \Phi(\mathbf{x})$  does depend on the gauge; we consider the scalar product of the field and its *solenoidal zero-mean* space-periodic vector potential  $\Phi(\mathbf{x}) = -\nabla^{-2}(\nabla \times \mathbf{f}(\mathbf{x}))$ , where  $\nabla^{-2}$  denotes the inverse Laplace operator.

Six families of steady solenoidal zero-mean flows  $\mathbf{w}$ ,  $2\pi$ -periodic in each Cartesian coordinate, that have zero vorticity helicity,  $\mathbf{w} \cdot (\nabla \times \mathbf{w}) = 0$ , were constructed in [9]. For such a field  $\mathbf{w}$ , obviously, the flow

$$\mathbf{v} = \beta \nabla \times \mathbf{w} \quad (3)$$

has a zero velocity helicity  $\mathcal{H}_v$ ; here  $\beta > 0$  is a normal-

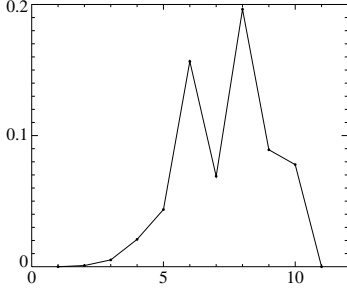


FIG. 1. Helicity spectrum seminorms  $\sum_{M-1 < |\mathbf{m}| \leq M} |H_{\mathbf{m}}(\mathbf{v})|$  (vertical axis) vs  $M$  (horizontal axis) for a sample flow (3) constructed for a potential  $\mathbf{w}$  from family L [9] (see the definition in section III).

ization factor such that the r.m.s. flow velocity of (3) is 1. To construct numerical examples, we use sample flows (13) for vector potentials  $\mathbf{w}$  from families  $V_1, V_2, L$  (14) (see section III) and flows (24) for vector potentials  $\mathbf{w}$  from family C (25) (see section V). Since the helicity spectrum (2) of fields  $\mathbf{w}(\mathbf{x}) = \sum_{\mathbf{m}} \hat{\mathbf{w}}_{\mathbf{m}} e^{i\mathbf{m} \cdot \mathbf{x}}$  from families C,  $V_1$  and  $V_2$  vanishes [9], the helicity spectrum of the respective flow (3) is zero as well: for any  $\mathbf{m}$ ,

$$H_{\mathbf{m}}(\mathbf{v}) = \overline{i\mathbf{m} \times \hat{\mathbf{w}}_{\mathbf{m}}} \cdot (i\mathbf{m} \times (i\mathbf{m} \times \hat{\mathbf{w}}_{\mathbf{m}})) = |\mathbf{m}|^2 H_{\mathbf{m}}(\mathbf{w}) = 0.$$

For a sample flow (3) used here for computations, where the potential  $\mathbf{w}$  belongs to family L, see Fig. 1. Family P flows were defined *ibid.* as poloidal flows whose scalar vector potential satisfies a certain partial differential equation. We do not consider potentials  $\mathbf{w}$  from family P, since the curl of any poloidal field is toroidal and hence the respective flow (3) is planar, and by the Zeldovich [14] antidynamo theorem such flows are incapable of the dynamo action.

The paper is organized as follows. In the next section we briefly review the standard multiscale expansion yielding expressions for the tensors of the magnetic  $\alpha$ -effect and eddy diffusivity in the limit of high scale separation. In sections III and V we present results of computation of the dominant growth rates of large-scale harmonically amplitude-modulated magnetic modes generated by the action of the  $\alpha$ -effect and negative eddy diffusivity, respectively. In both cases, the growth rates may experience a singular behavior in the vicinity of the critical molecular diffusivity for the onset of the small-scale dynamo action. In the presence of negative eddy diffusivity, this phenomenon is well-known (see sec. 3.7 in [15]). In the presence of the  $\alpha$ -effect, it was first noticed and qualitatively explained in [9]. In the present computations we observe, that at the critical molecular diffusivity the magnetic induction operator has a Jordan normal form cell of size 2 associated with the zero eigenvalue. Based on this observation, in section IV we develop formal asymptotic expansions of the eigenmodes and the associated eigenvalues of the magnetic induction operator in power series in  $\varepsilon^{1/2}$ , where  $\varepsilon > 0$  is the scale ratio. Finally, in section VI we draw conclusions of the present study.

## II. GROWTH RATES OF LARGE-SCALE MAGNETIC MODES

We explore numerically dynamos employing the  $\alpha$ -effect or negative eddy diffusivity for generation of large-scale harmonically amplitude-modulated magnetic modes

$$\mathbf{b} = e^{i\mathbf{q} \cdot \mathbf{x}} \mathbf{B}(\mathbf{x}, \varepsilon),$$

where the scale ratio  $\varepsilon > 0$  is small,  $|\mathbf{q}| = 1$  and  $\mathbf{B}(\mathbf{x}, \varepsilon)$  has the same space periodicity as the flow (their growth rates were calculated in [9], see also [15] for a detailed presentation). The eigenvalue of the magnetic induction operator

$$\mathbf{L} : \mathbf{b} \mapsto \eta \nabla^2 \mathbf{b} + \nabla \times (\mathbf{v} \times \mathbf{b})$$

associated with the large-scale mode is denoted by  $\lambda(\mathbf{q})$ . Here  $\eta$  is the magnetic molecular diffusivity and  $\text{Re } \lambda$  the growth rate of the magnetic mode  $\mathbf{b}$  (a negative growth rate actually indicates that the associated mode is decaying). The mode is solenoidal,

$$\nabla \cdot \mathbf{b} = 0, \quad (4)$$

and the fluid is supposed to be incompressible,  $\nabla \cdot \mathbf{v} = 0$ .

We now briefly review the relevant results of the multiscale analysis, derived by expanding a large-scale mode and the associated eigenvalue in power series in  $\varepsilon$ ,

$$\mathbf{b} = \sum_{n=0}^{\infty} \mathbf{b}_n(\mathbf{X}, \mathbf{x}) \varepsilon^n, \quad (5.1)$$

$$\lambda = \sum_{n=0}^{\infty} \lambda_n \varepsilon^n. \quad (5.2)$$

The  $\alpha$ -effect tensor  $\mathfrak{A}$  is a  $3 \times 3$  matrix, whose  $k$ th column is  $\mathfrak{A}_k = \langle \mathbf{v} \times \mathbf{S}_k \rangle$ , where  $\mathbf{S}_k$  are  $2\pi$ -periodic zero-mean solutions to three auxiliary problems

$$\mathbf{L} \mathbf{S}_k = - \frac{\partial \mathbf{v}}{\partial x_k} \quad \Leftrightarrow \quad \mathbf{L}(\mathbf{S}_k + \mathbf{e}_k) = 0, \quad (6)$$

$$\langle \mathbf{f} \rangle = (2\pi)^{-3} \int_{\mathbb{T}^3} \mathbf{f}(\mathbf{X}, \mathbf{x}) \mathbf{x} = \sum_{k=1}^3 \langle \mathbf{f} \rangle_k \mathbf{e}_k$$

denotes the spatial mean over the fast variables  $\mathbf{x}$  (i.e., over the periodicity cell  $\mathbb{T}^3$ ), and  $\mathbf{e}_k$  are unit vectors of the Cartesian coordinate system.

In the presence of the  $\alpha$ -effect, the leading order term in the expansion (5.2) of the eigenvalue  $\lambda(\mathbf{q})$  is  $\varepsilon \lambda_1(\mathbf{q})$ ; the respective maximum large-scale growth rate in the slow time  $T_1 = \varepsilon t$  is

$$\gamma_{\alpha} = \sqrt{\max(\alpha_1 \alpha_2, \alpha_2 \alpha_3, \alpha_1 \alpha_3)}, \quad (7)$$

where  $\alpha_i$  are eigenvalues of the symmetrized tensor  ${}^s \mathfrak{A}$ ,

$${}^s \mathfrak{A}_i^j = (\mathfrak{A}_i^j + \mathfrak{A}_j^i)/2.$$

For parity-invariant flows (i.e.,  $\mathbf{v}(\mathbf{x}) = -\mathbf{v}(-\mathbf{x})$ ),  $\mathfrak{A} = 0$  implying  $\gamma_{\alpha} = 0$  and  $\lambda(\mathbf{q}) = \varepsilon^2 \lambda_2(\mathbf{q}) + O(\varepsilon^3)$ . The large-scale generating mechanism is eddy diffusivity. The eddy

diffusivity tensor

$$\mathfrak{D}_{mk}^l = \left\langle \mathbf{Z}_l \cdot \left( 2\eta \frac{\partial \mathbf{S}_k}{\partial x_m} + \mathbf{e}_m \times (\mathbf{v} \times (\mathbf{S}_k + \mathbf{e}_k)) \right) \right\rangle \quad (8)$$

involves three zero-mean solutions  $\mathbf{Z}_l$  to auxiliary problems  $\mathbf{L}^* \mathbf{Z}_l = \mathbf{v} \times \mathbf{e}_l$  for the adjoint operator

$$\mathbf{L}^* : \mathbf{b} \mapsto \eta \nabla^2 \mathbf{b} - \mathbf{v} \times (\nabla \times \mathbf{b}). \quad (9)$$

It is easy to see that

$$\mathbf{Z}_k = \eta^{-1} \nabla^{-2} (\mathbf{v} \times (\mathbf{S}_k^- + \mathbf{e}_k)), \quad (10)$$

where  $\mathbf{S}_k^-$  denotes the solution to the problem (6) stated for the reverse flow  $-\mathbf{v}$ . The large-scale growth-rate in the slow time  $T_2 = \varepsilon^2 t$  is  $\text{Re } \lambda_{2\pm}(\mathbf{q}) + \mathcal{O}(\varepsilon)$ , where

$$\lambda_{2\pm}(\mathbf{q}) = -\eta - \frac{1}{2} \sum_{j,l,n} (D_n^l - D_l^n) q_j \pm \sqrt{d}, \quad (11.1)$$

$$d = \sum_{j,l,n} \left( ((^s D_n^l)^2 - ^s D_l^l {}^s D_n^n) q_j^2 - 2q_j q_n (^s D_n^l {}^s D_j^l - ^s D_l^l {}^s D_j^n) \right), \quad (11.2)$$

both sums are over even permutations of indices 1, 2 and 3 (i.e.,  $\epsilon_{jln} = 1$ , where  $\epsilon_{jln}$  is the unit antisymmetric tensor) and

$$D_n^l = \sum_m \mathfrak{D}_{mn}^l q_m, \quad {}^s D_n^l = (D_n^l + D_l^n)/2. \quad (11.3)$$

The minimum eddy diffusivity is defined as

$$\eta_{\text{ed}} = \min_{|\mathbf{q}|=1} (-\text{Re } \lambda_{2\pm}(\mathbf{q})). \quad (12)$$

The fields  $\mathbf{S}_k$  (6) and the dominant small-scale magnetic modes and their growth rates have been computed by the code [16] implementing the standard pseudo-spectral method. Typically, we have used the resolution of  $128^3$  Fourier harmonics, however, for the smallest magnetic molecular diffusivities considered here the double resolution computations with  $256^3$  harmonics have been performed. The energy spectrum of all fields used to construct graphs in Figs. 3 and 5 decays by at least 4 orders of magnitude.

### III. $\alpha$ -EFFECT IN FLOWS OF ZERO HELICITY

We have computed the maximum growth rates  $\gamma_\alpha$  (7) of large-scale modes generated by the action of the  $\alpha$ -effect in three sample flows (3),

$$\mathbf{v}^{\text{V}_1}(\mathbf{x}) = \beta^{\text{V}_1} (\dot{U}_1 (C_3 U_3 \ddot{U}_2 - C_2 U_2 \ddot{U}_3), \quad (13.1)$$

$$\dot{U}_2 (C_1 U_1 \ddot{U}_3 - C_3 U_3 \ddot{U}_1), \dot{U}_3 (C_2 U_2 \ddot{U}_1 - C_1 U_1 \ddot{U}_2),$$

$$\mathbf{v}^{\text{V}_2}(\mathbf{x}) = \beta^{\text{V}_2} (U_1 (C_3 \dot{U}_2 - C_2 \dot{U}_3), \quad (13.2)$$

$$U_2 (C_1 \dot{U}_3 - C_3 \dot{U}_1), U_3 (C_2 \dot{U}_1 - C_1 \dot{U}_2)),$$

$$\mathbf{v}^{\text{L}}(\mathbf{x}) = \beta^{\text{L}} \nabla A \times \nabla B, \quad (13.3)$$

(the coefficients  $\beta > 0$  normalize the flows so that the r.m.s. flow velocity is unity) for vector potentials from families  $\text{V}_1$ ,  $\text{V}_2$  and  $\text{L}$  [9],

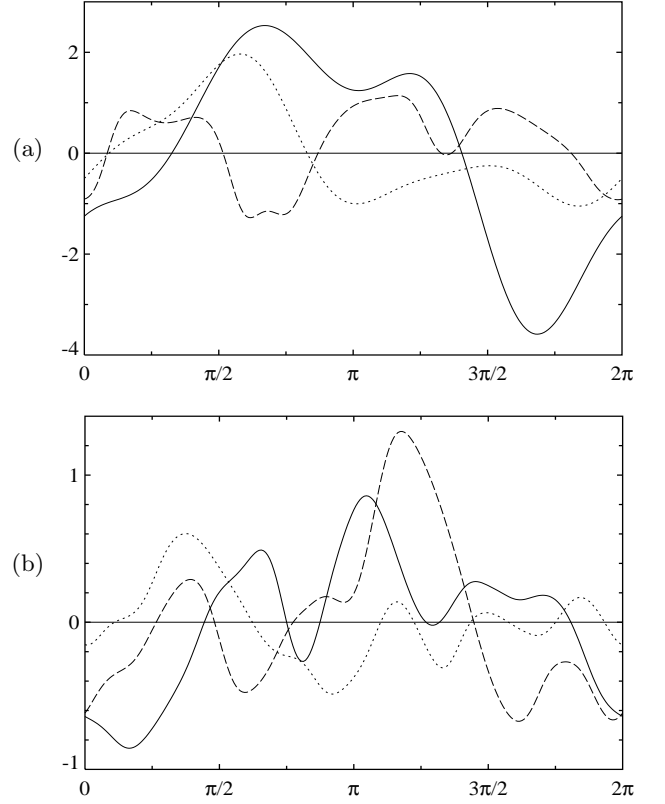


FIG. 2. Graphs of  $U_1$  (solid lines),  $U_2$  (dashed lines) and  $U_3$  (dotted lines, vertical axes) as functions of the respective Cartesian coordinate variable  $x_i$  (horizontal axis) used to construct the zero velocity helicity sample flows (13.1) and (13.2) for  $\text{V}_1$  (a) and  $\text{V}_2$  (b) family potentials  $\mathbf{w}$  (see (3)), (14.1) and (14.2), respectively.

$$\mathbf{w}^{\text{V}_1}(\mathbf{x}) = (C_1 U_1 \dot{U}_2 \dot{U}_3, C_2 \dot{U}_1 U_2 \dot{U}_3, C_3 \dot{U}_1 \dot{U}_2 U_3), \quad (14.1)$$

$$\mathbf{w}^{\text{V}_2}(\mathbf{x}) = (C_1 U_2 U_3, C_2 U_1 U_3, C_3 U_1 U_2), \quad (14.2)$$

$$\mathbf{w}^{\text{L}}(\mathbf{x}) = (A \nabla B - B \nabla A)/2, \quad (14.3)$$

respectively. Here  $C_i$  are arbitrary constants (satisfying  $C_1 + C_2 + C_3 = 0$  in (13.1) and (14.1));  $U_i$  are arbitrary smooth  $2\pi$ -periodic functions of  $x_i$  (at least two of which are zero-mean in (13.2));  $A$  and  $B$  are eigenfunctions of the Laplace operator associated with the same eigenvalue; dots denote differentiation of  $U_i$  in  $x_i$ . We have employed the family  $\text{V}_1$  flow considered in [9] (see (62) in that paper) to construct a sample flow (13.1) (the constitutive functions  $U_i(x_i)$  are shown in Fig. 2(a)). In our sample flow (13.2),  $U_i$  are random-coefficient sums of 20 Fourier harmonics whose energy spectra decay by 3 orders of magnitude (see Fig. 2(b)). In (13.3), the functions  $A$  and  $B$  are random-coefficient linear combinations of 72 Fourier harmonics that are eigenfunctions of the Laplacian associated with the eigenvalue  $-26$ . Their wave vectors are  $(\pm 3, \pm 4, \pm 1)$  and  $(\pm 5, 0, \pm 1)$ , and those obtained from these vectors by component permutations; the value  $-26$  has been chosen as the smallest one for which there exist two such triads of wave numbers.

For the same flows and molecular magnetic diffusivities  $\eta$ , we have computed the maximum growth rates  $\gamma_{\text{sm}}$  of zero-mean small-scale magnetic modes (i.e., eigenfunc-

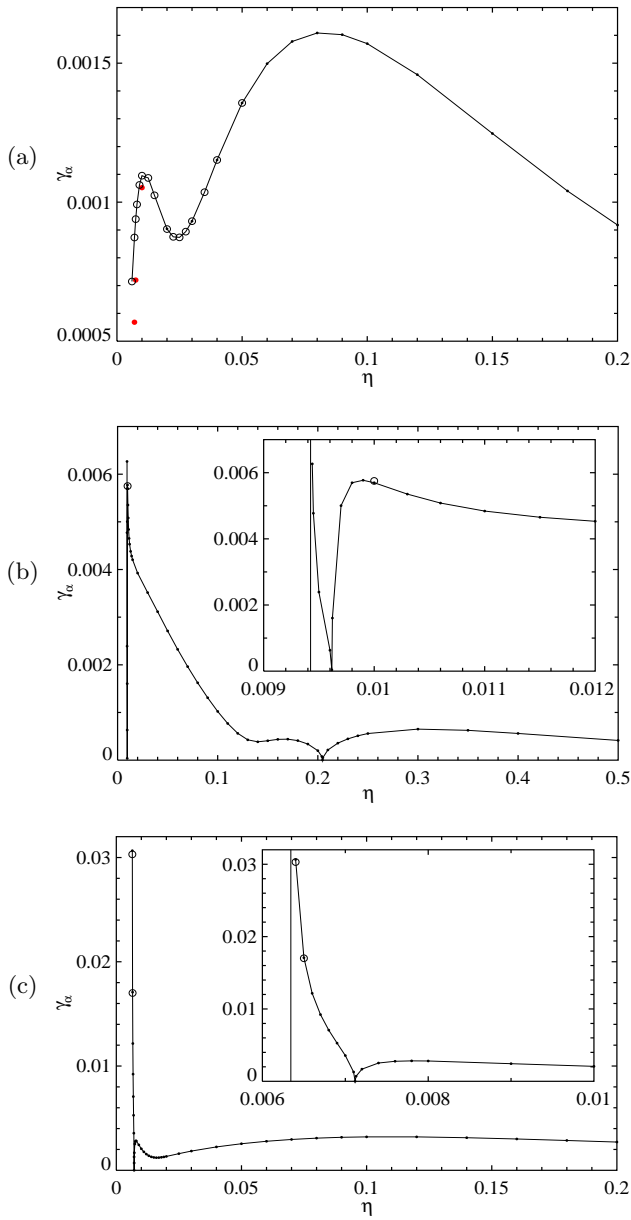


FIG. 3. Maximum slow-time growth rates (7) of large-scale modes generated by the  $\alpha$ -effect in sample flows (3) of zero velocity helicity for  $\mathbf{w}$  from families  $V_1$  (a),  $V_2$  (b) and  $L$  (c) as functions of the molecular diffusivity  $\eta$ . Insets in panels (b) and (c) show zooms of the graphs near the critical diffusivity (indicated by thin vertical lines) for the onset of the small-scale dynamo action. The resolution of computations is  $128^3$  (solid dots) or  $256^3$  (hollow circles) Fourier harmonics. Large solid dots (red in the electronic version of the paper) in (a) show computations in which the  $128^3$  harmonics resolution is insufficient.

tions of the magnetic induction operator  $\mathbf{L}$  that have the same spatial periodicity as the flow) and checked that no small-scale dynamos operate simultaneously with our  $\alpha$ -effect dynamos.

The behavior of  $\gamma_\alpha$  on varying molecular diffusivity  $\eta$  in the three flows is drastically different. While for flows  $\mathbf{v}^{V_2}$  (see Fig. 3(b)) and  $\mathbf{v}^L$  (Fig. 3(c)) the maximum slow-time growth rates increase to infinity when  $\eta$  approaches

from above the critical diffusivity  $\eta = \eta^{\text{cr}}$  for the onset of the small-scale field generation, for  $\mathbf{v}^{V_1}$  (Fig. 3(a)) it decays on decreasing  $\eta$  (although this trend cannot be guaranteed to persist for  $\eta$  smaller than those shown). By (7),  $\gamma_\alpha = 0$  when the intermediate eigenvalue  $\alpha_2$  of the symmetrized tensor  ${}^s\mathfrak{A}$  vanishes; the graphs feature cusps of the form  $(\eta - \eta^{\text{cr}})^{1/2}$  around such points. This occurs for  $\mathbf{v}^L$  once, for  $\mathbf{v}^{V_2}$  twice, but never for  $\mathbf{v}^{V_1}$ . Such peculiarities in the behavior of the maximum growth rates were also observed for flows of zero vorticity helicity in [9]. Fig. 3(c) attests that  $\gamma_\alpha$  can change significantly under a tiny variation of  $\eta$ .

#### IV. SINGULARITIES OF THE $\alpha$ -EFFECT GROWTH RATES AT THE ONSET OF THE SMALL-SCALE DYNAMO

Our computations show that there exists a critical molecular diffusivity  $\eta = \eta^{\text{cr}} > 0$  for the onset of the small-scale dynamo. For this  $\eta$ , a small-scale zero-mean mode  $\mathbf{S}_0$  emerges in the kernel of  $\mathbf{L}$ :

$$\mathbf{L}\mathbf{S}_0 = 0, \quad \langle \mathbf{S}_0 \rangle = 0.$$

We observe that for the critical diffusivity, the maximum growth rate of large-scale magnetic modes generated by the  $\alpha$ -effect has a singularity. As often in physics, this indicates that near this diffusivity the original expansions (5) of the mode and the associated eigenvalue break down, and we will now investigate this. At first sight, emergence of the new neutral short-scale mode requires introducing a new amplitude for this mode and increasing the number of solvability conditions. However, it is also necessary to take into account the possibility of emergence of Jordan normal form cell associated with the eigenvalue zero in the short-scale magnetic induction operator. Apart from these issues, the general course of actions remains the same as in the general problem [15]: The size of the Jordan form cell implies the form of the power series in which the large-scale mode and the associated eigenvalue of the large-scale magnetic induction operator are expanded. From the eigenvalue equation expanded in the power series, we deduce a hierarchy of equations for successive terms in the series for the mode and the associated eigenvalue. These elliptic equations in the fast variables are considered in consecutive order. First, the solvability conditions are verified; this yields differential equations in the slow variables for successive terms in the expansion of the mean field. Second, we construct solutions to the equations in the short-scale variables in terms of solutions to short-scale auxiliary problems. In principle, all terms in the expansions can be found this way, but we stop upon deriving a closed eigenvalue equation for the leading-order terms in the expansions of the mean magnetic mode and the associated eigenvalue.

Any eigenfunction  $\mathbf{b}$  of  $\mathbf{L}$  (i.e.,  $\mathbf{L}\mathbf{b} = \lambda\mathbf{b}$ ), as well as any generalized one (such that  $\mathbf{L}^m\mathbf{b} = \lambda\mathbf{b}$  for an integer  $m > 0$ ) has a non-zero mean only for  $\lambda = 0$ . However, space-periodic eigenfunctions (including generalized

ones) of any elliptic operator constitute a basis in the Lebesgue space of vector fields of the same spatial periodicity. Thus, for  $\eta = \eta^{\text{cr}}$  the (possibly generalized) kernel of  $\mathbf{L}$  involves at least 3 other (possibly generalized) eigenfunctions  $\mathbf{S}_k$  ( $k = 1, 2, 3$ ) such that  $\langle \mathbf{S}_k \rangle$  constitute a basis in  $\mathbb{R}^3$ .

Evidently, the kernel of the adjoint operator (9) involves 3 constant vector fields  $\mathbf{S}_k^* = \mathbf{e}_k$ ,  $k = 1, 2, 3$ . The dimensions of the generalized kernels of  $\mathbf{L}$  and its adjoint coincide, as well as the Jordan normal form structures of the two operators. Therefore, for  $\eta = \eta^{\text{cr}}$  there exists a zero-mean possibly generalized eigenfunction  $\mathbf{S}_0^*$  in the kernel of  $\mathbf{L}^*$ , such that  $\mathbf{L}^* \mathbf{S}_0^* = \mathbf{Q}$ , where  $\mathbf{Q}$  is a constant vector. Two possibilities arise:  $\mathbf{Q} = 0$ , any eigenfunction of  $\mathbf{L}$  or  $\mathbf{L}^*$  constituting an invariant subspace of the respective operator (there are no generalized eigenfunctions in the two kernels), or  $\mathbf{Q} \neq 0$ , in which case each operator has two size 1 Jordan form cells and one size 2 cell, associated with the eigenvalue 0. Computations confirm that the latter possibility realizes and that the dimension of the generalized kernel of  $\mathbf{L}$  generically is four:

$$\mathbf{L} \mathbf{S}_k = 0, \quad k = 0, 1, 2; \quad \mathbf{L} \mathbf{S}_3 = \mathbf{S}_0; \quad (15.1)$$

$$\langle \mathbf{S}_0 \rangle = 0, \quad \langle \mathbf{S}_k \rangle \quad (k = 1, 2, 3) \text{ constitute a basis in } \mathbb{R}^3; \quad (15.2)$$

$$\mathbf{L}^* \mathbf{S}_k^* = 0, \quad \mathbf{S}_k^* = \mathbf{e}_k \quad (k = 1, 2, 3); \quad (15.3)$$

$$\mathbf{L}^* \mathbf{S}_0^* = \mathbf{Q} \neq 0, \quad \langle \mathbf{S}_0^* \rangle = 0. \quad (15.4)$$

We proceed to explore this case.

We assume henceforth in this section  $\eta = \eta^{\text{cr}}$  and make no assumptions concerning the velocity (or any other) helicity. The results that we obtain here are applicable whenever the generalized kernel of the small-scale magnetic induction operator  $\mathbf{L}$  is four-dimensional, and the operator involves a  $2 \times 2$  Jordan normal form cell associated with the eigenvalue 0, whereby there exist the fields  $\mathbf{S}_k$  and  $\mathbf{S}_k^*$  with the properties (15).

The solvability condition for a problem  $\mathbf{L} \mathbf{b} = \mathbf{f}$  is the orthogonality of the r.h.s. to the (non-generalized) kernel of the adjoint operator in the functional Lebesgue space, which amounts to  $\langle \mathbf{f} \rangle = 0$  (this follows from the Fredholm alternative theorem for linear problems with compact operators).

In contrast with (5), the presence of the Jordan cell requires considering expansions of a large-scale mode and the associated eigenvalue in power series in  $\varepsilon^{1/2}$  [17, 18]:

$$\mathbf{b} = \sum_{n=0}^{\infty} \hat{\mathbf{b}}_n(\mathbf{X}, \mathbf{x}) \varepsilon^{n/2}, \quad (16.1)$$

$$\lambda = \sum_{n=0}^{\infty} \hat{\lambda}_n \varepsilon^{n/2}. \quad (16.2)$$

Substituting them into the eigenvalue equation  $\mathbf{L} \mathbf{b} = \lambda \mathbf{b}$  yields a hierarchy of equations at successive orders  $\varepsilon^n$ :

$$\begin{aligned} \mathbf{L} \hat{\mathbf{b}}_n + 2\eta(\nabla \cdot \nabla_{\mathbf{X}}) \hat{\mathbf{b}}_{n-2} + \nabla_{\mathbf{X}} \times (\mathbf{v} \times \hat{\mathbf{b}}_{n-2}) + \eta \nabla_{\mathbf{X}}^2 \hat{\mathbf{b}}_{n-4} \\ = \sum_{m=0}^n \hat{\lambda}_{n-m} \hat{\mathbf{b}}_m. \end{aligned} \quad (17)$$

Here the subscript  $\mathbf{X}$  marks differential operators in slow variables; the magnetic induction operator  $\mathbf{L}$  is henceforth assumed to involve differentiation in fast variables  $\mathbf{x}$  only. The solenoidality condition (4) at order  $\varepsilon^{n/2}$  yields an equation, whose mean and fluctuating parts are

$$\nabla_{\mathbf{X}} \cdot \langle \hat{\mathbf{b}}_n \rangle = 0, \quad (18.1)$$

$$\nabla_{\mathbf{x}} \cdot \hat{\mathbf{b}}_n + \nabla_{\mathbf{X}} \cdot \{\hat{\mathbf{b}}_{n-2}\} = 0. \quad (18.2)$$

*Order  $\varepsilon^0$  equation.* Under our assumptions, the relevant solution to the first equation in the hierarchy (17),

$$\mathbf{L} \hat{\mathbf{b}}_0 = \hat{\lambda}_0 \hat{\mathbf{b}}_0,$$

is

$$\hat{\mathbf{b}}_0 = \sum_{k=0}^2 c_{0k}(\mathbf{X}) \mathbf{S}_k(\mathbf{x}), \quad \hat{\lambda}_0 = 0.$$

*Order  $\varepsilon^{1/2}$  equation.* The solvability condition for the second equation,

$$\mathbf{L} \hat{\mathbf{b}}_1 = \hat{\lambda}_1 \hat{\mathbf{b}}_0,$$

states  $\langle \hat{\mathbf{b}}_0 \rangle = 0 \Rightarrow c_{01} = c_{02} = 0$  (since  $\langle \mathbf{S}_1 \rangle$  and  $\langle \mathbf{S}_2 \rangle$  are linearly independent). Thus,

$$\hat{\mathbf{b}}_1 = \sum_{k=0}^3 c_{1k}(\mathbf{X}) \mathbf{S}_k(\mathbf{x}),$$

where

$$c_{13} = \hat{\lambda}_1 c_{00}. \quad (19)$$

A natural condition  $\hat{\mathbf{b}}_0 \neq 0$  (of the normalization sense) implies  $\hat{\lambda}_1 \neq 0$ .

*Order  $\varepsilon$  equation* is

$$\mathbf{L} \hat{\mathbf{b}}_2 + 2\eta(\nabla \cdot \nabla_{\mathbf{X}}) \hat{\mathbf{b}}_0 + \nabla_{\mathbf{X}} \times (\mathbf{v} \times \hat{\mathbf{b}}_0) = \hat{\lambda}_2 \hat{\mathbf{b}}_0 + \hat{\lambda}_1 \hat{\mathbf{b}}_1. \quad (20)$$

In view of (19), its solvability condition,

$$\nabla_{\mathbf{X}} \times \langle \mathbf{v} \times \hat{\mathbf{b}}_0 \rangle = \hat{\lambda}_1 \langle \hat{\mathbf{b}}_1 \rangle,$$

is an eigenvalue-like problem for  $\hat{\lambda}_1$  and  $c_{13}$ :

$$\nabla_{\mathbf{X}} \times (\mathfrak{A} c_{13}) = \hat{\lambda}_1^2 \sum_{k=1}^3 \langle \mathbf{S}_k \rangle c_{1k}. \quad (21)$$

Here  $\mathfrak{A}$  denotes the tensor (actually, now a vector) of the magnetic  $\alpha$ -effect

$$\mathfrak{A} = \langle \mathbf{v} \times \mathbf{S}_0 \rangle.$$

This is consistent with Parker's [2] idea that the interaction of fine structures of a flow (here,  $\mathbf{v}$ ) and magnetic field (predominantly  $c_{00} \mathbf{S}_0$ ) gives rise to a mean e.m.f. ( $c_{00} \mathfrak{A}$ ) that may have a component, parallel to the large-scale mean magnetic field (predominantly  $\langle \hat{\mathbf{b}}_1 \rangle$ ).

To solve the problem (21), we assume that the large-scale mode is amplitude-modulated by a Fourier harmonic,

$$\mathbf{c}_1 = \mathbf{C} e^{i\mathbf{q} \cdot \mathbf{X}},$$

whereby

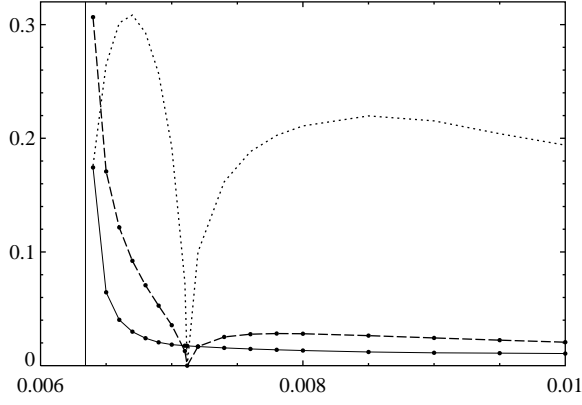


FIG. 4. Graphs of  $10 \max_{|\mathbf{q}|=1} \text{Re } \lambda_1(\mathbf{q})$  (dashed line),  $\max_{|\mathbf{q}|=1} \text{Im } \lambda_1(\mathbf{q})$  (solid line) and their ratio (dotted line) as functions of the molecular eddy diffusivity  $\eta$  (horizontal axis). Small circles show the computed values. Thin vertical line is the asymptote for the maximum growth rate  $\max_{|\mathbf{q}|=1} \text{Re } \lambda_1(\mathbf{q})$  located at the critical molecular diffusivity  $\eta = \eta^{\text{cr}}$ , for the onset of the small-scale dynamo.

$$i\mathbf{q} \times \mathfrak{A}C_3 = \hat{\lambda}_1^2 \sum_{k=1}^3 \langle \mathbf{S}_k \rangle C_k. \quad (22)$$

Here  $\mathbf{q}$  and  $\mathbf{C}$  are constant vectors,  $|\mathbf{q}| = 1$ . Scalar multiplying (22) by  $\langle \mathbf{S}_1 \rangle \times \langle \mathbf{S}_2 \rangle$  yields

$$\hat{\lambda}_1(\mathbf{q}) = \pm(1+i) \sqrt{\frac{(\mathbf{q} \times \mathfrak{A}) \cdot (\langle \mathbf{S}_1 \rangle \times \langle \mathbf{S}_2 \rangle)}{2(\langle \mathbf{S}_1 \rangle \times \langle \mathbf{S}_2 \rangle) \cdot \langle \mathbf{S}_3 \rangle}} \quad (23)$$

(by our assumptions, the denominator is non-zero). Evidently, there exists a growing mode ( $\text{Re } \hat{\lambda}_1 > 0$ ), unless the numerator vanishes; the maximum growth rate is

$$\max_{|\mathbf{q}|=1} \text{Re } \hat{\lambda}_1(\mathbf{q}) = \sqrt{\frac{|\mathfrak{A} \times (\langle \mathbf{S}_1 \rangle \times \langle \mathbf{S}_2 \rangle)|}{2|(\langle \mathbf{S}_1 \rangle \times \langle \mathbf{S}_2 \rangle) \cdot \langle \mathbf{S}_3 \rangle|}}.$$

Also, we determine from (22)

$$c_{1k} = \epsilon_{k,3-k,3} \frac{(\mathbf{q} \times \mathfrak{A}) \cdot (\langle \mathbf{S}_{3-k} \rangle \times \langle \mathbf{S}_3 \rangle)}{(\mathbf{q} \times \mathfrak{A}) \cdot (\langle \mathbf{S}_1 \rangle \times \langle \mathbf{S}_2 \rangle)} C_3$$

for  $k = 1, 2$ . The solenoidality of  $\langle \hat{\mathbf{b}}_1 \rangle$  (18.1) is equivalent to  $\mathbf{q} \cdot \sum_{k=1}^3 \langle \mathbf{S}_k \rangle c_{1k} = 0$ , that follows directly from (22).

We deduce from (23) that

$$\max_{|\mathbf{q}|=1} \text{Im } \hat{\lambda}_1(\mathbf{q}) = \max_{|\mathbf{q}|=1} \text{Re } \hat{\lambda}_1(\mathbf{q}).$$

This suggests that the ratio of the maximum real and imaginary parts of the dominant term  $\lambda_1$  in the expansion (5.2) of the eigenvalue for  $\eta > \eta^{\text{cr}}$  tends to unity when  $\eta \rightarrow \eta^{\text{cr}}$  from above. In order to test this hypothesis, we plot in Fig. 4 the real and imaginary parts of  $\lambda_1$  for the flow (13.3) considered in section III (the real part is multiplied by 10 in order to unify the vertical scales of the three graphs), as well as their ratio. Clearly, the ratio is far from the predicted limit value. This is not very surprising: The singular behavior of  $\text{Re } \lambda_1$  for  $\eta \rightarrow \eta^{\text{cr}}$  is

offset by shrinking to zero of the radius of convergence of the series (5.2). Branches of eigenvalues of the magnetic induction operator  $\lambda(\eta, \varepsilon, \mathbf{q})$  are continuous in the three quantities on which they depend. However, both the real and imaginary parts of  $\lambda$  tend to 0 when  $\varepsilon \rightarrow 0$ , and therefore there is no continuity at  $\varepsilon = 0$  of the ratios  $\text{Im } \lambda / \text{Re } \lambda$  or  $\max_{|\mathbf{q}|=1} \text{Im } \lambda / \max_{|\mathbf{q}|=1} \text{Re } \lambda$ .

Thus, from the equation for  $n = 2$  we obtain the leading-order term  $\hat{\lambda}_1 \varepsilon^{1/2}$  in the expansion of the eigenvalue, and large-scale amplitudes  $c_{1k}(\mathbf{X})$  for  $k = 1, 2, 3$  in the expansion of the large-scale mode  $\hat{\mathbf{b}}_1$ . The leading-order term  $\hat{\mathbf{b}}_1$  is now completely determined by (19) (up to the coefficient  $C_3$ , which is arbitrary because modes are defined up to a constant factor). The solvability condition for (20) being satisfied, we find from this equation the next term  $\hat{\mathbf{b}}_2$  up to an arbitrary field from  $\ker L$  and the eigenvalue expansion term  $\hat{\lambda}_2$ . Following essentially the same procedure, we can solve successively all equations (17), find all terms in the expansions (16) and establish that solenoidality conditions (18) are satisfied.

## V. NEGATIVE EDDY DIFFUSIVITY IN FLOWS OF ZERO VELOCITY HELICITY

We have computed the minimum magnetic eddy diffusivity (12) for flow (3)

$$v_1^C = \beta ((\mathbf{a} \cdot \mathbf{b})a_2 + n^2 b_2) \sin(\mathbf{a} \cdot \mathbf{x}) \quad (24.1)$$

$$+ ((\mathbf{a} \cdot \mathbf{b})b_2 + n^2 a_2) \sin(\mathbf{b} \cdot \mathbf{x}) \sin nx_3,$$

$$v_2^C = -\beta ((\mathbf{a} \cdot \mathbf{b})a_1 + n^2 b_1) \sin(\mathbf{a} \cdot \mathbf{x}) \quad (24.2)$$

$$+ ((\mathbf{a} \cdot \mathbf{b})b_1 + n^2 a_1) \sin(\mathbf{b} \cdot \mathbf{x}) \sin nx_3,$$

$$v_3^C = \beta n(a_1 b_2 - a_2 b_1)(\cos(\mathbf{a} \cdot \mathbf{x}) - \cos(\mathbf{b} \cdot \mathbf{x})) \cos nx_3, \quad (24.3)$$

$$\beta = 2((n^4 + (\mathbf{a} \cdot \mathbf{b})^2)(|\mathbf{a}|^2 + |\mathbf{b}|^2) + 2n^2((\mathbf{a} \cdot \mathbf{b})^2 + |\mathbf{a}|^2 |\mathbf{b}|^2))^{-1/2} \quad (24.4)$$

calculated for the family C “cosine” [9] potential

$$w_1^C = n(b_1 \sin(\mathbf{a} \cdot \mathbf{x}) + a_1 \sin(\mathbf{b} \cdot \mathbf{x})) \cos nx_3,$$

$$w_2^C = n(b_2 \sin(\mathbf{a} \cdot \mathbf{x}) + a_2 \sin(\mathbf{b} \cdot \mathbf{x})) \cos nx_3, \quad (25)$$

$$w_3^C = -(\mathbf{a} \cdot \mathbf{b})(\cos(\mathbf{a} \cdot \mathbf{x}) + \cos(\mathbf{b} \cdot \mathbf{x})) \sin nx_3,$$

where  $\mathbf{a} = (a_1, a_2, 0)$  and  $\mathbf{b} = (b_1, b_2, 0)$  are constant horizontal vectors. The flow (24) is parity-invariant relative points  $\mathbf{Q}_j = (0, 0, (j + 1/2)\pi/n)$  for all integer  $j$ .

The symmetries of (24) and (25) are the same, enabling us to apply the analysis [9] of the eddy diffusivity tensor structure. Since translation by  $\mathbf{a} = (\pi/n)\mathbf{e}_3$  reverses the flow,  $\mathbf{S}_n^-(\mathbf{x}) = \mathbf{S}_n(\mathbf{x} + \mathbf{a})$  for all  $n$ , and solving just the three auxiliary problems (6) suffices for computing the eddy diffusivity tensor  $\mathfrak{D}$  (8), (10). The translation antisymmetry implies  $\mathfrak{D}_{mk}^l = -\mathfrak{D}_{ml}^k$  for all  $l, m, k$  and  $\mathfrak{D}_{mk}^k = 0$ . Therefore,  ${}^s\mathbf{D} = 0$ , and for any wave vector  $\mathbf{q}$  eigenvalues (11) of the eddy diffusivity operator are real and two-fold. Moreover, the flow (24) is symmetric in  $x_3$  relative the points  $\mathbf{Q}_j$ , and therefore  $\mathfrak{D}_{mk}^l = 0$  if all

TABLE I. Primary flows (24) and (25) as small- and large-scale dynamos. Numbers of the primary cosine flows (24) and (25) (in parenthesis, from [9]) falling into the specified categories are shown.

	$\eta = 0.01$		$\eta = 0.02$	
	$\eta_{ed} < 0$	$\eta_{ed} > 0$	$\eta_{ed} < 0$	$\eta_{ed} > 0$
Small-scale dynamo	33 (61)	3 (12)	28 (27)	4 (4)
No small-scale dynamo	36 (25)	127 (85)	23 (20)	144 (132)

indices  $l, m, k$  do not exceed 2, or precisely two of them are equal to 3. Consequently,

$$\lambda_2(\mathbf{q}) = -\eta + \mathfrak{D}_{31}^2 q_3^2 + \mathfrak{D}_{12}^3 q_1^2 + (\mathfrak{D}_{22}^3 + \mathfrak{D}_{13}^1) q_1 q_2 + \mathfrak{D}_{23}^1 q_2^2,$$

and the minimum eddy diffusivity (12) is

$$\eta_{ed} = \eta - \max \left( \mathfrak{D}_{31}^2, \frac{1}{2} \left( \mathfrak{D}_{12}^3 + \mathfrak{D}_{23}^1 \right) + \sqrt{(\mathfrak{D}_{12}^3 - \mathfrak{D}_{23}^1)^2 + (\mathfrak{D}_{22}^3 + \mathfrak{D}_{13}^1)^2} \right). \quad (26)$$

Generation of small- and large-scale fields was investigated in [9] for a set of 183 “primary” sample flows (25) satisfying the following conditions: 1) the horizontal vectors  $\mathbf{a} = (a_1, a_2, 0)$  and  $\mathbf{b} = (b_1, b_2, 0)$  have integer components such that  $|a_i| \leq 3$ ,  $|b_i| \leq 3$ , and  $n \leq 3$  is a positive integer; 2) the largest common divisor of the four numbers  $a_1, a_2, b_1, b_2$  is 1; 3) the flows are non-planar (by the Zeldovich [14] antidynamo theorem planar flows are irrelevant as non-dynamos); 4) no primary flow can be mapped into another one by reflections and their combinations. Applying the same rules, here we have selected for numerical study a set of 199 primary flows (24) (the number has increased, because in contrast to (25), flows (24) for orthogonal  $\mathbf{a}$  and  $\mathbf{b}$  are non-planar).

The distributions of the dominant fast-time growth rates of small-scale magnetic modes and of the minimum eddy diffusivity computed for the primary flows (24) for  $\eta = 0.01$  and  $0.02$  are shown in Fig. 5 (see also Table I) in comparison with the similar distributions for the normalized primary flows (25). More than a half of the primary flows (24) (for  $\eta = 0.01$ , roughly 1.5 times more than for (25)) are neither small-, nor large-scale dynamos. For both sets, the second largest category are flows that can generate both small- and large-scale fields. While a comparable number of flows of our prime interest is found that are incapable of small-scale generation but feature negative eddy diffusivity, only a few flows in which eddy diffusivity is positive can generate small-scale fields. In Fig. 5, the growth rates concentrate significantly closer to the origin for flows (24) than for (25), although, unlike the flows (25), some flows (24) feature for  $\eta = 0.01$  a strong negative eddy diffusivity; the small respective growth rates of small-scale fields suggest that for them  $\eta = 0.01$  is close to the critical value for the onset of the small-scale generation.

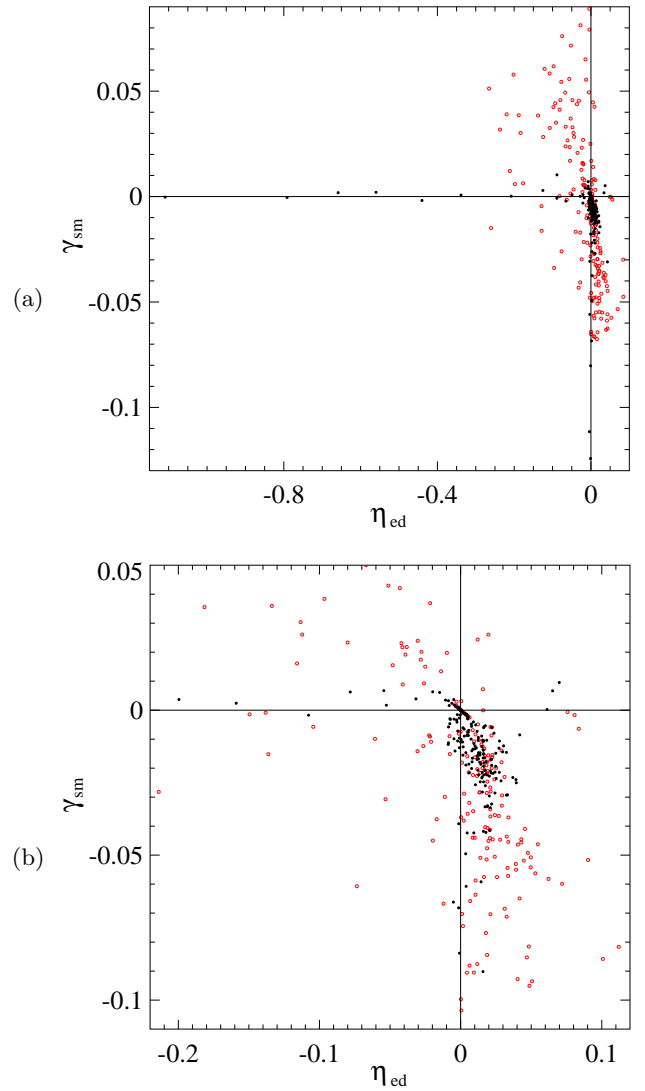


FIG. 5. Dominant growth rates  $\gamma_{sm}$  of small-scale modes versus minimum eddy diffusivity (26) in the primary cosine flows (24) (filled circles) and (25) (hollow circles, red in the electronic version of the paper) for  $\eta = 0.01$  (a) and  $0.02$  (b).

## VI. CONCLUDING REMARKS

We have considered kinematic dynamos powered by steady flows, whose velocity helicity density vanishes in every point in space. The flows employed in simulations, (13) and (24), have been constructed as normalized curls (3) of space-periodic steady solenoidal flows  $\mathbf{w}$ , whose vorticity helicity (in other words, kinetic helicity) is pointwise zero; these  $\mathbf{w}$  belong to four analytically defined families  $V_1, V_2, L$  (14) and  $C$  (25) introduced in [9]. All flows studied here have an identically zero helicity spectrum, except for  $\mathbf{v}^L$  (13.3) (see Fig. 1). Generation of large-scale fields has been investigated in the limit of high scale separation by computing the magnetic  $\alpha$ -effect or eddy diffusivity tensors formerly derived by applying the multiscale formalism (see, e.g., [15]). We have established that both mechanisms generate large-scale magnetic field and a significant part of the employed flows

generate small-scale field for the considered molecular diffusivities (corresponding to moderate local magnetic Reynolds numbers below 200). This is our main finding: kinematic generation of small- or large-scale magnetic field does not require flows to have a non-zero velocity helicity or helicity spectrum. This reinforces the skepticism of [9] concerning the ability of any helicity-like quantity to characterize reliably the flow efficiency as a dynamo.

We observe a fast increase, from 0 to  $\infty$ , of the maximum (over the direction of the large-scale wave vector  $\mathbf{q}$ ) large-scale growth rate due to the action of the  $\alpha$ -effect,  $\gamma_\alpha$ , under a tiny variation of molecular eddy diffusivity decreasing from  $\eta = 0.007118$  (for which the intermediate eigenvalue of the symmetrized  $\alpha$ -tensor vanishes) to  $\eta^{\text{cr}} = 0.006342$  (the critical diffusivity for the onset of the small-scale dynamo action), see Fig. 3(c). Let us note that (like in the case of infinitely negative eddy diffusivity), this does not imply an unphysical singular behavior of the large-scale dynamo: When the  $\alpha$ -effect tensor is non-zero (the generic case), it determines the leading-order term in the expansion in the scale ratio  $\varepsilon$  of an eigenvalue of the large-scale magnetic induction operator,  $\lambda = \sum_{n=0}^{\infty} \lambda_n \varepsilon^n$ . This term is  $\varepsilon \lambda_1$ , where  $\lambda_1$  is an eigenvalue of the magnetic  $\alpha$ -effect operator  $\mathbf{b} \mapsto \nabla_{\mathbf{x}}(\mathbf{2b})$ . However, the power series has a finite radius of convergence apparently tending to zero for  $\eta \rightarrow \eta^{\text{cr}}$ , so that  $\lambda$

remains finite or even tends to zero. As we have shown in section IV, the relevant expansion of  $\lambda$  at  $\eta = \eta^{\text{cr}}$  is in the power series in  $\sqrt{\varepsilon}$ . The expansion has revealed that this large-scale dynamo has an unusual feature: the amplitude of the mean magnetic field is order  $\sqrt{\varepsilon}$  smaller than the amplitude of the fluctuating component of the field.

The dynamos explored here are slow: Fluid particle trajectories for flows (13.1) and (13.2) have first integrals  $\sum_{m=1}^3 \int (C_m U_m / \dot{U}_m) \dot{\mathbf{x}}_m$  and  $\sum_{m=1}^3 \int (C_m / U_m) \dot{\mathbf{x}}_m$ , respectively, and for flow (13.3) two first integrals  $A$  and  $B$ . For a flow (24), the trajectories belong to vertical surfaces, whose intersections with horizontal planes satisfy the differential equation which is the ratio of (24.1) and (24.2). This is incompatible with a chaotic behavior of the trajectories required for fast dynamos [19, 20]. An interesting mathematical problem is to construct a pointwise non-helical steady flow acting as fast dynamo (or at least lacking global first integrals).

## ACKNOWLEDGMENTS

RC was supported by the project POCI-01-0145-FEDER-006933/SYSTEC financed by ERDF through COMPETE 2020 and by FCT (Portugal). The authors would like to thank the anonymous Referee, whose comments helped us to significantly improve the paper.

- 
- [1] Moffatt H.K., Ricca R.L. Helicity and the Călugăreanu invariant. *Proc. R. Soc. Lond. A*, **439**, 411–429 (1992).
  - [2] Parker E.N. Hydrodynamic dynamo models. *Astrophys. J.* **122**, 293–314 (1955).
  - [3] Moreau J.-J. Constantes d’un îlot tourbillonnaire en fluide parfait barotrope. *C. R. hebdomadaire. Acad. Sci. Paris*, **252**, 2810–2813 (1961).
  - [4] Moffatt H.K. The degree of knottedness of tangled vortex lines. *J. Fluid Mech.* **35**, 117–129 (1969).
  - [5] Moffatt H.K., Proctor M.R.E. The role of the helicity spectrum function in turbulent dynamo theory. *Geophys. Astrophys. Fluid Dynamics*, **21**, 265–283 (1982).
  - [6] Stepanov R., Plunian F. Kinematic dynamo in a tetrahedron of Fourier modes. *Fluid Dyn. Res.*, **50**, 051409 (2018).
  - [7] Zheligovsky V.A., Galloway D.J. Dynamo action in Christopherson hexagonal flow. *Geophys. Astrophys. Fluid Dynamics*, **88**, 277–293 (1998).
  - [8] Gilbert A.D., Frisch U., Pouquet A. Helicity is unnecessary for alpha effect dynamos, but it helps. *Geophys. Astrophys. Fluid Dynamics*, **42**, 151–161 (1988).
  - [9] Rasskazov A., Chertovskih R., Zheligovsky V. Magnetic field generation by pointwise zero-helicity three-dimensional steady flow of incompressible electrically conducting fluid. *Phys. Rev. E*, **97**, 043201 (2018).
  - [10] Moffatt H.K. Magnetic field generation in electrically conducting fluids. CUP, 1978.
  - [11] Krause F., Rädler K.-H. Mean-field magnetohydrodynamics and dynamo theory. Academic-Verlag, Berlin, 1980.
  - [12] Moffatt H.K. Helicity and singular structures in fluid dynamics. *PNAS*, **111** (10), 3663–3670 (2014).
  - [13] Rädler K.-H., Brandenburg A.  $\alpha$ -effect dynamos with zero kinetic helicity. *Phys. Rev. E*, **77**, 026405 (2008).
  - [14] Zeldovich Ya.B. The magnetic field in the two-dimensional motion of a conducting turbulent fluid. *Journ. Exper. Theor. Phys.* **31**, 154–156 (1956). Engl. transl.: *Sov. Phys. J.E.T.P.* **4**, 460–462 (1957).
  - [15] Zheligovsky V.A. Large-scale perturbations of magnetohydrodynamic regimes: linear and weakly nonlinear stability theory. *Lecture Notes in Physics*, vol. 829, Springer-Verlag, Heidelberg, 2011.
  - [16] Zheligovsky V. Numerical solution of the kinematic dynamo problem for Beltrami flows in a sphere. *J. Scientific Computing*, **8**, 41–68 (1993).
  - [17] Kato T. Perturbation theory for linear operators. Springer-Verlag, Berlin, 1966.
  - [18] Vishik M.M. Periodic dynamo. II. In: Numerical modelling and analysis of geophysical processes (Computational seismology, iss. 20). Keilis-Borok V.I., Levshin A.L. (eds.), 12–22. Nauka, Moscow, 1987. Engl. transl.: *Computational seismology*, **20**, 10–21. Allerton Press, NY, 1988.
  - [19] Vishik M.M. Magnetic field generation by the motion of a highly conducting fluid. *Geophys. Astrophys. Fluid Dynamics*, **48**, 151–167 (1989).
  - [20] Klapper I., Young L.S. Rigorous bounds on the fast dynamo growth rate involving topological entropy. *Communications Math. Phys.* **173**, 623–646 (1995).